

Neuroprotective effects of meloxicam on transient brain ischemia in rats: the two faces of anti-inflammatory treatments

Irene Fernández Ugidos^{1,†}, Paloma González-Rodríguez¹, María Santos-Galdiano^{1,2}, Enrique Font-Belmonte^{1,‡}, Berta Anuncibay-Soto^{1,§}, Diego Pérez-Rodríguez^{1,||}, José Manuel Gonzalo-Orden^{1,3}, Arsenio Fernández-López^{1,†}

<https://doi.org/10.4103/1673-5374.367846>

Date of submission: August 23, 2022

Date of decision: December 6, 2022

Date of acceptance: December 12, 2022

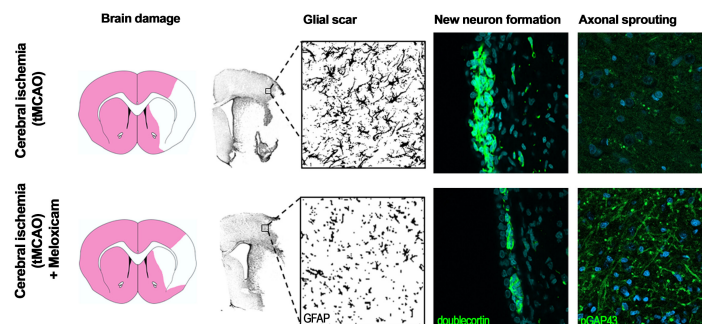
Date of web publication: January 30, 2023

From the Contents

Introduction	1961
Methods	1962
Results	1963
Discussion	1964

Graphical Abstract

Meloxicam treatment modulates glial scar reactivity, new neuron formation, and axonal sprouting



Abstract

The inflammatory response plays an important role in neuroprotection and regeneration after ischemic insult. The use of non-steroidal anti-inflammatory drugs has been a matter of debate as to whether they have beneficial or detrimental effects. In this context, the effects of the anti-inflammatory agent meloxicam have been scarcely documented after stroke, but its ability to inhibit both cyclooxygenase isoforms (1 and 2) could be a promising strategy to modulate post-ischemic inflammation. This study analyzed the effect of meloxicam in a transient focal cerebral ischemia model in rats, measuring its neuroprotective effect after 48 hours and 7 days of reperfusion and the effects of the treatment on the glial scar and regenerative events such as the generation of new progenitors in the subventricular zone and axonal sprouting at the edge of the damaged area. We show that meloxicam's neuroprotective effects remained after 7 days of reperfusion even if its administration was restricted to the two first days after ischemia. Moreover, meloxicam treatment modulated glial scar reactivity, which matched with an increase in axonal sprouting. However, this treatment decreased the formation of neuronal progenitor cells. This study discusses the dual role of anti-inflammatory treatments after stroke and encourages the careful analysis of both the neuroprotective and the regenerative effects in preclinical studies.

Key Words: anti-inflammatories; astrocyte; axonal sprouting; cylinder test; doublecortin; focal brain ischemia; glial scar; inflammation; neuroprotection; new neuron generation; transient stroke

Introduction

Inflammation plays a major role in many central nervous system diseases and a crucial role in neuroprotection and regeneration after stroke (Paciaroni et al., 2009; Anrather and Iadecola, 2016; Jayaraj et al., 2019). Post-ischemic inflammation is triggered by free radicals and damage-associated molecular patterns produced by dying neurons and involves the production of cytokines, the activation of microglia and astroglia cells, the infiltration of peripheral immune cells into the brain, and in later events, the formation of a glial scar surrounding the damaged area (Kaur et al., 2020; Pluta et al., 2021; Jiang et al., 2022). These events activate positive pro-inflammatory feedback that exacerbates tissue damage (Tsuyama et al., 2018; Otani and Shichita, 2020; Pluta et al., 2021). The inflammatory response initiated as a consequence of a brain insult is maintained long-term (Sekeljic et al., 2012; Radenovic et al., 2020) and interacts with neurogenesis and neuronal repair after stroke (Tsuyama et al., 2018; Franklin and Simons, 2022; Passarelli et

al., 2022). In this regard, the interaction between inflammation and the regenerative response has been widely studied, and whether it is beneficial or detrimental is still a matter of debate (Dabrowski et al., 2019; Pluta et al., 2021). The extensive role of the inflammatory process in early and late events after stroke has led to the search for agents that modulate this pro-inflammatory loop as a putative palliative and regenerative strategy (Drieu et al., 2018).

A key step in the inflammatory response is the activation of cyclooxygenases (COX). The isoform COX-2 has been historically targeted because it is highly inducible after stroke, compared to the isoform COX-1, which is considered to be constitutively expressed (Faki and Er, 2021). Moreover, excessive COX-1 inhibition has been related to peripheral side effects (Saad and Mathew, 2022) driving pharmaceutical companies to develop selective COX-2 inhibitors (Cruz et al., 2022; Ju et al., 2022). In this regard, the use of non-steroidal anti-inflammatory drugs (NSAIDs) that block either COX-1, COX-2, or both of them

¹Área de Biología Celular, Instituto de Biomedicina, Campus de Vegazana s/n, Universidad de León, León, Spain; ²Neural Therapies SL. Edif. Institutos de Investigación. Planta baja. Local B43. Campus de Vegazana s/n. León, Spain; ³Department of Medicina, Cirugía y Anatomía Veterinaria, University of León, León, Spain

†Current address: Department of Pharmacology, Tulane University School of Medicine, New Orleans, LA, USA

‡Current address: Department of Neurology, David Geffen School of Medicine at University of California (UCLA), Los Angeles, CA, USA

§Current address: Department of Life Sciences, Imperial College London (ICL), London, UK

||Current address: Department of Clinical and Movement Neurosciences, UCL Queen Square Institute of Neurology, London, UK

*Correspondence to: Arsenio Fernández-López, PhD, aferl@unileon.es.

<https://orcid.org/0000-0001-5557-2741> (Arsenio Fernández-López)

Funding: This work was supported by MINECO and FEDER funds: ref CPP2021-008855 and RTC-2015-4094-1, Junta de Castilla y León ref. LE025P17, and Neural Therapies SL, ref. NT-Dev-01 (all to AFL and JMGO).

How to cite this article: Ugidos IF, González-Rodríguez P, Santos-Galdiano M, Font-Belmonte E, Anuncibay-Soto B, Pérez-Rodríguez D, Gonzalo-Orden JM, Fernández-López A (2023) Neuroprotective effects of meloxicam on transient brain ischemia in rats: the two faces of anti-inflammatory treatments. *Neural Regen Res* 18(9):1961-1967.

to various extent has been widely discussed. NSAIDs are not expensive, and their kinetics have been very well characterized. However, their effects after stroke are controversial. The general belief that the highly COX-2 selective blockers would improve neuroprotection resulted in controversy when several studies showed a detrimental effect in different models of ischemia (Kunz et al., 2002; Pu et al., 2007; Anunciabay-Soto et al., 2018; Stiller and Hjendahl, 2022), leading to the reconsideration of both the role of COX-1 inhibition in post-ischemic treatments as well as the proper balance of the inhibition of both isoforms (Choi et al., 2009; Ugidos et al., 2017; Ghazanfari et al., 2021).

Meloxicam is a preferential COX-2 inhibitor that exhibits COX-2 specificity between 3 and 77 times that of COX-1 (Pairet et al., 1998; Hawkey, 1999) and is widely used in the veterinary clinic (Horgan et al., 2020; Schoos et al., 2020; Pereira et al., 2021), as well as in humans (Dadasheva et al., 2020; Dixit et al., 2020). Meloxicam is widely used as a post-operative treatment to reduce inflammation and pain with very efficient results (Bekker et al., 2018). There are just a few studies showing the potential of meloxicam as a short-term palliative agent after focal ischemia (Gupta et al., 2002; Jacobsen et al., 2013). However, there are no studies showing the differential effect of the meloxicam dosage on the neuroprotective effect, or the long-term effects of meloxicam treatment in neuroprotection and in regenerative events after stroke. This study is the first to investigate the short- and long-term neuroprotective effects of meloxicam in a focal ischemia model with a special focus on the impact of meloxicam on regenerative events after 7 days of reperfusion and provides a frame to discuss the relevance of the anti-inflammatory dosage in the balance between inflammation and regeneration.

Methods

Animals

Sixty-four 8-week-old male Sprague-Dawley rats (320–360 g) (Janvier Labs, Le Genest-Saint-Isle, France) were used to perform this study. Only males were used to avoid the already described sexually dimorphic inflammatory response to stroke (Banerjee and McCullough, 2022). Animals were housed at standard temperature ($22 \pm 1^\circ\text{C}$) in a 12-hour light/dark cycle with food (Panlab, Barcelona, Spain) and water *ad libitum*. Animals were caged in pairs and randomly allocated to the different experimental groups by a different person than those who performed the surgery.

Fifty animals were used to run the study. Five animals died during surgery. Three animals were discarded due to a lack of reperfusion after surgery. Four animals were also discarded because of insufficient blood flow restriction, and two animals were culled due to poor outcomes after stroke.

All procedures were carried out in compliance with the Animal Research: Reporting of *In Vivo* Experiments (ARRIVE) guidelines (Percie du Sert et al., 2020), and the Guidelines of the European Union Council (63/2010/EU) following the Spanish regulation (RD53/2013) for the use of laboratory animals and were approved by the Scientific Committee of the University of Leon (approval date: June 4, 2020). All efforts were made to minimize animal suffering and to reduce the number of animals used.

Surgery and drug administration

Transient middle cerebral artery occlusion (tMCAO) was performed as described previously (Shahjouei et al., 2016; Ugidos et al., 2017; Santos-Galdiano et al., 2018). Briefly, anesthesia was induced with 3.5–4% isoflurane (Esteve, Barcelona, Spain) in 100% O₂-enriched air with a flow of 2 L/min and maintained at 2% isoflurane during the surgery. The body temperature was maintained at $36 \pm 1^\circ\text{C}$ during surgery with a feedback-regulated heating pad monitored with a rectal probe. A Doppler probe (Perimed, Järfälla, Sweden) was fixed on the temporal bone over the MCA to monitor blood flow. Once the carotid bifurcation was exposed, a 4-0 silicon-coated monofilament (Doccol Corporation, Sharon, MA, USA) was inserted into the right common carotid artery and led through the right internal carotid artery until blocking of the origin of the MCA. Blood flow blockage was monitored by a Doppler probe to ensure at least 80% reduction in blood flow. One hour after occlusion, the monofilament was withdrawn, allowing blood reperfusion while monitoring by a Doppler probe, and incisions were permanently sutured. The same surgery was performed in sham animals, except for MCA occlusion with the monofilament. No analgesic drugs were administered to avoid a bias in the interpretation of the data. The dose-response assay of meloxicam was performed by administering 0.5 mg/kg (Mel0.5), 1 mg/kg (Mel1), 5 mg/kg (Mel5), and 10 mg/kg (Mel10) of meloxicam (Boehringer Ingelheim, Ingelheim am Rhein, Germany) intravenously (i.v.) through the tail vein, 1 and 24 hours after reperfusion. Meloxicam was prepared by diluting the stock (5 mg/ml) to an adequate concentration with sterile saline to achieve an adequate volume of injection that ranges between 150–250 μL , to avoid hypervolemic stress. A comparable volume of vehicle (saline) was administered to vehicle (Veh) and sham animals (Sham). For studies with a longer time of reperfusion (7 days), meloxicam 1 mg/kg was administered in the acute phase (1 and 24 hours after reperfusion, i.v.; Mel1-a) or as a chronic dose (one hour after reperfusion and then a repeated dose every 24 hours until sacrifice, i.v.; Mel1-c). For all the studies, animals were randomized before the surgery intervention by a computer-assigned randomized number method. The experimental design is represented in **Figure 1**.

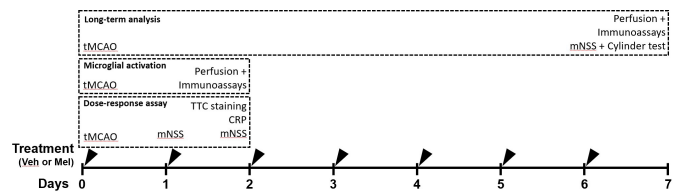


Figure 1 | Experimental design.

CRP: C-reactive protein; Mel: meloxicam; mNSS: modified neurological severity score; tMCAO: transient middle cerebral artery occlusion; TTC: 2,3,5-triphenyl tetrazolium chloride. Black arrows indicate treatment (vehicle [Veh] or meloxicam [Mel]).

Behavioral analysis

The neurological deficit was evaluated based on the modified Neurological Severity Score (mNSS) (Senda et al., 2011) at 24 hours, 48 hours, and 7 days after reperfusion. For this, rats were video recorded with a recording camera (Canon, Tokyo, Japan) for 5 minutes on a behavioral table and then were evaluated by two blinded and independent observers. Results are shown as the average given by the two researchers at each time point.

The cylinder test was performed after 7 days of reperfusion to evaluate stroke impact on motor performance. The rats were placed in a plastic cylinder (37.5 cm high 13 cm diameter) and filmed for 10 minutes. A blinded observer scored the first 20 forelimb contacts with the cylinder. The use of the contralateral (contacts made with the contralateral paw) over the ipsilateral (contacts made with the ipsilateral forepaw) was calculated as the bias on the contralateral using the following formula: $\text{bias (\%)} = 100 \times (\text{contralateral contacts}) / (\text{ipsilateral contacts} + \text{contralateral contacts})$ (Trueman et al., 2017).

Infarct volume

After 48 hours of ischemia, rats were euthanized by decapitation, and their brains were removed and placed in a cold rodent brain matrix (ASI Instruments, Warren, MI, USA). Coronal 2 mm-thick sections were obtained and incubated in 1% 2,3,5-triphenyl tetrazolium chloride (TTC) (Thermo Fisher Scientific, Waltham, MA USA) in 50 mM phosphate-buffered saline (PBS), pH 7.4 for 25 minutes at 37°C . Then, sections were fixed in 4% paraformaldehyde (PFA) in PBS overnight. Brain sections were digitized at 600 dpi resolution (Canon), and infarct volume was measured with ImageJ software release 1.52k (NIH, Bethesda, MD, USA, RRID: SCR_003070). Infarct volume was calculated as $\text{Infarct volume (\%)} = \text{non-stained volume (mm}^3\text{)} / \text{total volume (mm}^3\text{)} \times 100$.

C-reactive protein

Blood was collected from the heart with a 21G syringe at the moment of the sacrifice and centrifuged immediately at $1200 \times g$ for 10 minutes at 4°C . The serum was aliquoted and stored at -80°C until further use. C-reactive protein (CRP) was measured by an ELISA kit (Cat# CYT294, MilliporeSigma, Burlington, MA, USA) following the manufacturer's instructions.

Immunofluorescence and image acquisition

Rats were sacrificed with a sublethal dose of sodium pentobarbital (200 mg/kg) (Esteve, Barcelona, Spain) and were perfused via the aorta with 4% PFA. Brains were fixed, cryoprotected in 30% sucrose in PBS, and sectioned. Seven equidistant 40- μm coronal sections separated by 1 mm between bregma +2.20 mm and bregma -3.8 mm (Paxinos and Watson, 2006) were used for neuronal nuclear protein (NeuN) staining to obtain a representative coverage of the ischemic damage to represent the ischemic volume. Three sections separated by 1 mm between bregma +1.2 and bregma -0.8 (Paxinos and Watson, 2006) were used for the analysis of different markers in the ischemic penumbra and subventricular zone (SVZ), which include: ionized calcium-binding adapter molecule 1 (IBA-1) as a marker for microglia, glial fibrillary acidic protein (GFAP) as a marker for reactive astrocytes, phosphorylated growth-associated protein 43 (pGAP43) as a marker for axonal sprouting, and doublecortin (DCX) as a marker for immature neurons. Primary and secondary antibodies are summarized in **Table 1**. A Zeiss LSM 800 confocal microscope (Zeiss, Oberkochen, Germany) was used to acquire images from the immunostained sections. Bias in the image quantification was avoided by keeping constant the pinhole, detector gain, laser power, and pixel dwell during acquisition.

Microglia analysis

A modification of the optical disector method (Gundersen et al., 1988) was used to count IBA1⁺ cells and perform morphometric and densitometric analyses. In brief, a grid of 0.255 mm² squares with a lateral resolution of 0.156 $\mu\text{m}/\text{pixel}$ was acquired with a Plan-Apochromat 40x/1.30Oil DIC (UV) VIS-IR M27. In each disector, Z-stack images were taken separated by 4 μm along the Z-axis (5 images, 20 μm in total). IBA-1⁺ cells were counted in each disector, and the average of the disectors in each rat was expressed as the number of IBA-1⁺ cells/mm³. The degree of microglial activation was estimated by applying a skeletonization filter in ImageJ (Morrison and Filosa, 2013) to obtain the number of branches (expressed as 'number of endpoints') and the total length of the branches (expressed as 'summed process length' or 'branch



Table 1 | Antibodies and specific conditions used in immunofluorescence assays

Primary antibody	Blocking agent	Incubation solution	Secondary antibody
Goat anti IBA-1, 1:2000 (Abcam, Cambridge, MA, USA, Cat# ab5076, RRID: AB_2224402), incubation for 16 h at 4°C	BSA 1%	Triton X100 (Thermo Fisher Scientific, Waltham, MA USA) 0.2% in PBS	Alexa fluor 647 donkey anti-goat, 1:500 (Thermo Fisher Scientific, Cat# A21448, RRID: AB_10374882)
Rabbit anti GFAP, 1:500 (Dako, Agilent, Cat# Z0334, RRID: AB_10013382), incubation for 16 h at 4°C	Goat serum 20%	Triton X100 0.2% in PBS	Alexa fluor 488 donkey anti-goat, 1:500 (Molecular Probes, Cat# A-11055, RRID: AB_2534102)
Mouse anti NeuN, 1:500, (Millipore, Burlington, MA, USA, Cat# MAB337, RRID: AB_2313673), incubation for 16 h at 4°C	Goat serum 20%	Triton X100 0.2% in PBS	Alexa fluor 568 goat anti-mouse, 1:500 (Thermo Fisher Scientific, Cat# A21069, RRID: AB_10563601)
Rabbit anti DCX, 1:500 (Cell Signaling Technology, Danvers, MA, USA, Cat# 4604, RRID: AB_561007), incubation for 16 h at 4°C	Goat serum 20%	Triton X100 0.2% in PBS	Alexa fluor 488 donkey anti-goat, 1:500 (Molecular Probes, Cat# A-11055, RRID: AB_2534102)
Rabbit anti pGAP43, 1:500 (Abcam, Cat# ab194929, RRID: AB_2925212), incubation for 16 h at 4°C	Goat serum 20%	Triton X100 0.5% in PBS	Alexa fluor 488 donkey anti-goat, 1:500 (Molecular Probes, Cat# A-11055, RRID: AB_2534102)

All tissues were exposed to an antigen retrieval solution (citrate buffer pH 6.0) for 25 minutes at 95°C. Secondary antibodies were incubated at room temperature for 90 minutes. DAPI was used to contrast nuclei in immunofluorescence assays. DCX: Doublecortin; GFAP: glial fibrillary acidic protein; IBA-1: ionized calcium-binding adapter molecule 1; pGAP43: phosphorylated growth-associated protein 43.

length') in each dissector, and this value was divided by the number of IBA-1⁺ cells to obtain the endpoints/cell and the summed process length/cell.

Neuronal loss quantification

For NeuN staining, each section was scanned to obtain a high-resolution image (1.25 μm/pixel) of the whole section using the Tile Scan Module (included in Zen Blue software) with a Plan-Apochromat 10x/0.45 M27 objective. Some parts of the damaged tissue were lost during processing due to the massive stroke damage. Thus, to avoid bias, whole section images were overlapped with the corresponding coronal section of the Paxinos Rat Brain Atlas (+2.2, +1.2, +0.2, -0.8, -1.8, -2.8, -3.8 AP) (Paxinos and Watson, 2006). The area considered as "neuronal loss" was defined as the lack of clear neuronal bodies and measured with Image J software. Results were expressed as the percentage of neuronal loss = (non-stained area/total analyzed area) × 100.

Glial scar analysis

Z-stack images were acquired separated by 320 μm between them (distance between the center of each image), setting the first image in the edge of the glial scar. The total fluorescence intensity (TFI) was obtained to normalize the total relative amount of GFAP per cell. TFI values were normalized using the number of astrocytes in each dissector and the average TFI for each rat was expressed as TFI/cell.

Axonal sprouting analysis

Z-stack images were obtained on the edge of the ischemic damage. pGAP43 staining was used to create a binary mask based on an intensity threshold. Mean fluorescence intensity was measured as a representation of the average relative protein amount in each analyzed region.

Neuronal progenitor analysis

Z-stack images were obtained from the SVZ, as well as different regions of the striatum located perpendicular to the SVZ were imaged. The area stained with DCX was measured with ImageJ in each dissector. The average values per rat in each analyzed region are expressed as DCX⁺ area/mm³.

Statistical analysis

Statistical analyses were carried out using GraphPad Prism 6 (GraphPad Software, San Diego, CA, USA, www.graphpad.com). Student's *t*-test was used to compare data between two different groups when only two groups are considered. One-way analysis of variance (ANOVA) followed by Tukey's test was performed to analyze the differences between treatments in parametric datasets. Two-way ANOVA followed by Tukey's *post hoc* was performed to analyze the effect of the treatments in different areas when different distances were considered. The global effect of distance/treatment when analyzing astrocytic GFAP and DCX was obtained from the two-way ANOVA, and the individual comparisons were obtained from Tukey's *post hoc*

analysis. Non-parametric behavioral test values were analyzed by Kruskal-Wallis test followed by Dunn's *post hoc* tests. Unless otherwise indicated, data are presented as mean ± SEM. Individual dots in plots represent individual biological replicates (animals) in each experimental group. Significance was set at *P* < 0.05.

Results

Intermediate doses of meloxicam reduce the infarct volume and improve post-ischemic behavior after 48 hours of reperfusion

To set up the optimal neuroprotective dose of meloxicam, a dose-response assay measuring the infarct volume after 48 hours of reperfusion was performed (Figure 2A). The different dosages displayed a U-shaped curve where the neuroprotective effects reached statistical significance at 1 mg/kg of meloxicam (Mel1) (Veh vs. Mel1, *P* = 0.0132). Consistently, behavioral data at both 24 and 48 hours after reperfusion only displayed significant improvement for 1 mg/kg of meloxicam (Veh 24 h vs. Mel1 24 h, *P* = 0.0371; Veh 48 h vs. Mel1 48 h, *P* = 0.040) (Figure 2B). Representative brain slices stained with TTC are observed in Figure 2C.

After 48 hours of reperfusion, the levels of CRP were used to measure systemic inflammation in plasma. The range of doses assayed showed a U-shaped curve and only animals treated with 1 and 5 mg/kg of meloxicam reached significantly lower CRP levels than vehicle animals (Veh vs. Mel1, *P* = 0.0039; Veh vs. Mel5, *P* = 0.0375) (Figure 2D). To corroborate the anti-inflammatory effect, the microglia activation in the ischemic hemisphere (ipsilateral) was only measured after the administration of the neuroprotective dose (1 mg/kg of meloxicam). The total branch length and endpoints of IBA-1⁺ cells significantly increased in treated animals (Veh vs. Mel1, *P* = 0.010 and *P* = 0.02 respectively) (Figures 2E and F, respectively). No changes in the number of IBA-1⁺ cells were detected (Veh vs. Mel1, *P* = 0.385) (Figure 2G).

Neuroprotection remains after 7 days of reperfusion in both acute and chronic treatments with meloxicam

To determine if neuroprotection exerted by 1 mg/kg is maintained after 7 days of reperfusion, we measured the extent of the stroke using the absence of neurons as a proxy of damaged regions after acute (Mel1-a) and chronic (Mel1-c) treatments with meloxicam (Figure 3A and E). Neuronal loss observed in vehicle animals was decreased by the acute and chronic treatments with meloxicam (Veh vs. Mel1-a, *P* = 0.0247; Veh vs. Mel1-c, *P* = 0.0017; Figure 3B). Acute and chronic treatments presented similar results. The behavior analysis using the mNSS revealed no differences between vehicle and treated animals (Figure 3C). However, animals chronically treated with meloxicam displayed improved motor behavior in the cylinder test compared to vehicle animals (Veh vs. Mel1-c, *P* = 0.0138), but not acutely treated animals (Veh vs. Mel1-a, *P* = 0.2754; Figure 3D).

The reactivity of the astrocytes in the glial scar is modulated by both chronic and acute treatments with meloxicam

Astrocytes at the edge of the cortical glial scar showed a hypertrophic morphology characterized by engrossed cell bodies with wide branches, which were observed from 80 to 400 μm from the border of the injury and were progressively replaced by less hypertrophied cells further from the edge (Figure 4A, C, and D). The reactivity of astrocytes in the glial scar was quantified as the levels of GFAP immunoreactivity per cell (TFI/cell). This analysis revealed a distance-dependent decrease in the astrocyte reactivity (*F*_(5, 83) = 5.36, *P* = 0.0003), attenuated by meloxicam treatment (*F*_(2, 83) = 18.02; *P* < 0.0001; Figure 4B).

Meloxicam treatment enhances axonal sprouting after 7 days of reperfusion

Axonal sprouting was measured in the edge of the glial scar as a molecular parameter of the tissue's new connectivity attempt (Figure 5A) using pGAP43, a specific marker for axonal sprouting (Kawasaki et al., 2018). The analysis revealed that both chronic and acute treatment with meloxicam significantly increased the levels of pGAP43 after 7 days of reperfusion (Veh vs. Mel1-a, *P* = 0.0233; Veh vs. Mel1-c, *P* = 0.0272; Figure 5B and C).

Stroke-induced neurogenesis after 7 days is decreased by meloxicam

To analyze the effect of meloxicam in neurogenesis, we labeled the neuronal progenitor cells (NPCs) with DCX and analyzed them in both the SVZ (NPCs) and in the striatum (migrating NPCs) (Figure 6A). In general terms, the treatment with meloxicam significantly reduced the area occupied by DCX (two-way ANOVA treatment effect (Meloxicam effect, *P* = 0.004, *F*_(2,59) = 9.023). The area occupied by DCX cells in the SVZ (expressed as DCX⁺ area/mm³) was significantly lower in animals treated with an acute dose of meloxicam compared to vehicle animals (SVZ Veh vs. SVZ Mel1-a, *P* = 0.026). Chronic treatment with meloxicam also decreased the area of DCX cells in the SVZ, but we failed in finding significance (*P* = 0.069). The closest region to the SVZ analyzed also displayed significant reductions in meloxicam-treated animals (Veh vs. Mel1-a, *P* = 0.047; Veh vs. Mel1-c, *P* = 0.0261; Figure 6B). No differences were observed in the different conditions at 560, 880, and 1200 μm of distance from the SVZ (Figure 6C).

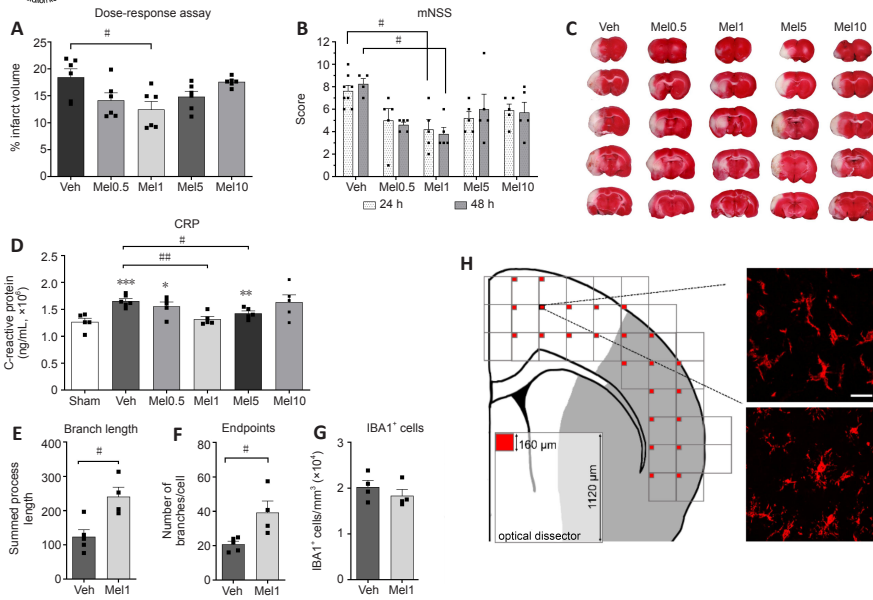


Figure 2 | Neuroprotective and anti-inflammatory effects of meloxicam after 48 hours of reperfusion. (A) Percentage of infarct volume in the dose-response assay after 48 hours of reperfusion ($n = 6$). (B) Neurological score measured at both 24 and 48 hours after reperfusion ($n = 4-8$). (C) Representative brain slices stained with TTC. White (or unstained) indicates infarcted regions. CRP levels in plasma (D; $n = 5$) and microglial activation measured as branch length (E), the number of endpoints (F), and the number of IBA-1⁺ cells (G; $n = 4-5$). (H) Schematic representation of image acquisition (red squares) by optical dissector method to measure microglial activation in the cerebral cortex and representative images of IBA-1⁺ cells (red). Data are presented as mean \pm SEM. One-way analysis of variance followed by Tukey's test for the TTC assay and CRP assay and followed by the Kruskal-Wallis test for the behavioral assay. # $P < 0.05$, ### $P < 0.01$, vs. vehicle-treated animals; * $P < 0.05$, ** $P < 0.01$, *** $P < 0.001$, vs. sham animals (Student's t -test). CRP: C-reactive protein; IBA-1: ionized calcium-binding adapter molecule; mNSS: modified neurological severity score; TTC: 2,3,5-triphenyl tetrazolium chloride.

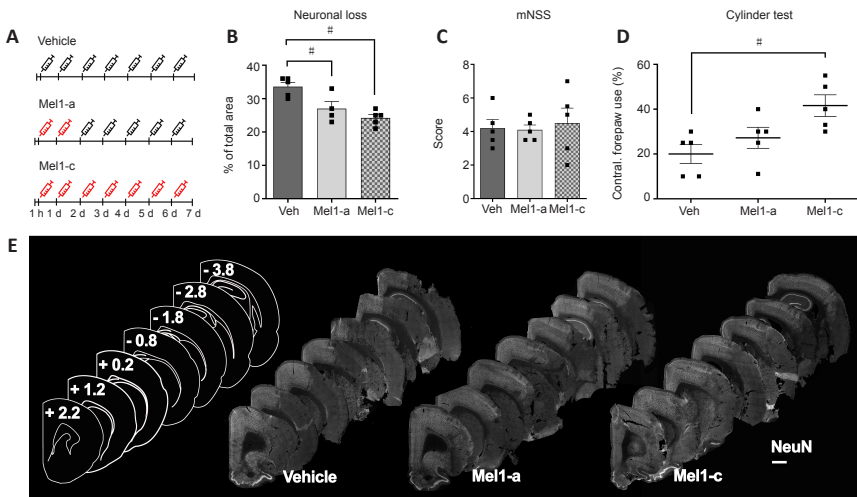


Figure 3 | Long-term neuroprotection of meloxicam treatment. (A) Schematic representation of meloxicam dosage at 7 days of reperfusion. Red syringes represent a meloxicam administration of 1 mg/kg and white syringes represent vehicle administration. (B) Percentage of neuronal loss after 7 days of reperfusion measured as the area without NeuN staining ($n = 5$). Behavioral analysis was assayed with mNSS (C) and the cylinder test (D; $n = 5$). (E) Representative sections of NeuN staining. Infarcted regions are observed as a lack of NeuN staining (dark grey) compared to the non-infarcted regions (light grey to white, showing defined neuronal cell bodies). Scale bar: 400 μ m. Mel1-a: Meloxicam 1 mg/kg was administered in the acute phase (1 and 24 hours after reperfusion, i.v.); Mel1-c: meloxicam 1 mg/kg was administered as a chronic dose (one hour after reperfusion and then a repeated dose every 24 hours until sacrifice, i.v.). # $P < 0.05$, vs. vehicle-treated animals. One-way analysis of variance followed by Tukey's *post hoc* test was performed to analyze neuronal loss and Kruskal-Wallis followed by Dunn's test to analyze the behavioral tests. mNSS: modified Neurological Severity Score; NeuN: neuronal nuclear protein.

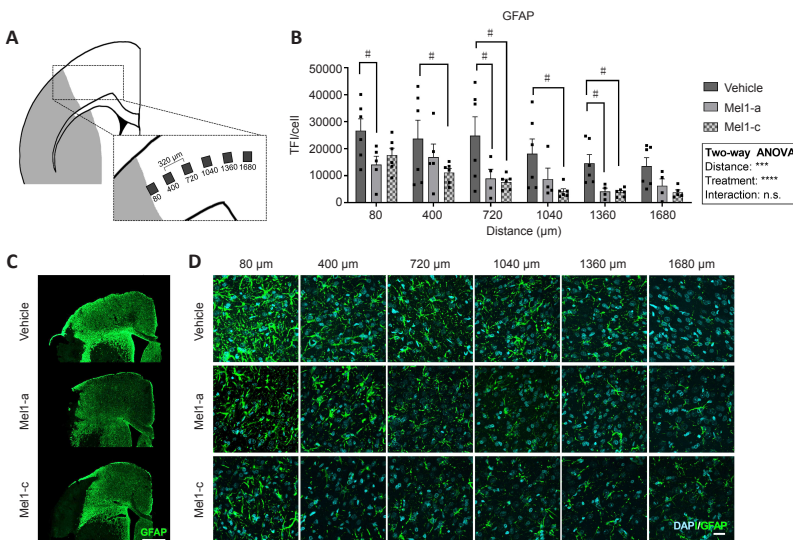


Figure 4 | Astrocyte reactivity in the glial scar in the cerebral cortex. (A) Representative scheme of the specifically analyzed regions in the glial scar. (B) GFAP TFI/cell at each point of analysis along the glial scar ($n = 5-6$). Representative images of GFAP immunostaining are shown as a whole image of the cerebral cortex (C) and each analyzed region (D). Scale bar: 200 μ m in C and 20 μ m in D. Mel1-a: Meloxicam 1 mg/kg was administered in the acute phase (1 and 24 hours after reperfusion, i.v.); Mel1-c: meloxicam 1 mg/kg was administered as a chronic dose (1 hour after reperfusion and then a repeated dose every 24 hours until sacrifice, i.v.). # $P < 0.05$, vs. vehicle-treated animals (two-way analysis of variance followed by Tukey's *post hoc* test). GFAP: Glial fibrillary acidic protein; TFI: total fluorescence intensity.

Discussion

The neuroprotective effect of meloxicam: more is not always better

Searching for an optimal meloxicam dose is an indispensable step since the balance of inflammation after stroke may increase the damage or provide a null effect in terms of neuroprotection. Our dose-response analysis revealed a U-shaped response in a short range of doses (from 0.5 mg/kg to 10 mg/kg).

Our results fit previous reports addressing a loss of COX-2 selectivity when meloxicam is administered at high doses (Pairet et al., 1998; Hawkey, 1999; Lascelles et al., 2005). We considered the possibility that meloxicam shows a hermetic response, a concept that includes the inverted U- or U-shaped curves in dose-response studies. This phenomenon has been explained as a limited, temporally-based overcompensation after a disruption in homeostasis and has been predicted to be nearly universal, although it is not observed

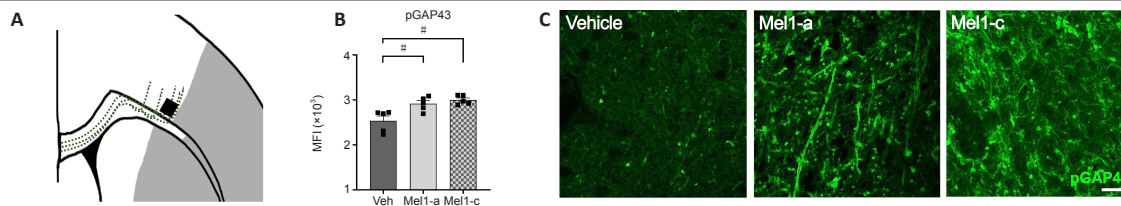


Figure 5 | Axonal sprouting after 7 days of reperfusion.

(A) Scheme showing the analyzed regions (gray squares) in the pGAP43 immunostaining. Dotted line represents one of the possible pathways described for axonal sprouting. (B) Immunoreactivity of pGAP43 expressed as the mean fluorescence intensity per mm² (n = 5) and (C) representative images of the pGAP43 immunostaining (scale bar: 20 μm). Mel1-a: Meloxicam 1 mg/kg was administered in the acute phase (1 and 24 hours after reperfusion, i.v.); Mel1-c: meloxicam 1 mg/kg was administered as a chronic dose (1 hour after reperfusion and then a repeated dose every 24 hours until sacrifice, i.v). #P < 0.05, vs. vehicle-treated animals (one-way analysis of variance followed by Tukey's *post hoc* test). MFI: mean fluorescence intensity; pGAP43: phosphorylated growth-associated protein 43.

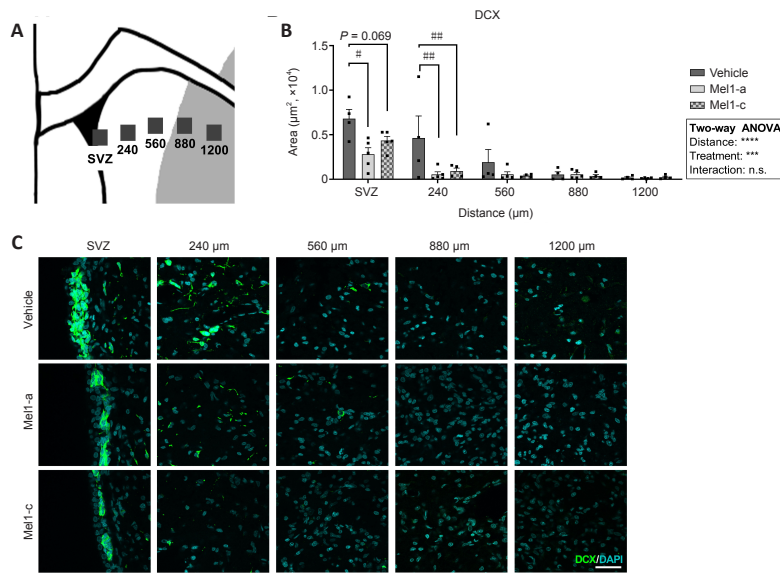


Figure 6 | Neuronal progenitors after 7 days of reperfusion.

(A) Scheme showing the analyzed regions (gray squares) in the DCX immunostaining. The numbers on the bottom of the gray squares represent the distance from the SVZ in μm. (B) Area occupied by DCX⁺ cells in the different analyzed regions. (C) the representative images of each analyzed region (scale bar: 20 μm) (n = 4–5). Mel1-a: Meloxicam 1 mg/kg was administered in the acute phase (1 and 24 hours after reperfusion, i.v.); Mel1-c: meloxicam 1 mg/kg was administered as a chronic dose (one hour after reperfusion and then a repeated dose every 24 hours until sacrifice, i.v). #P < 0.05, ##P < 0.01, vs. vehicle-treated animals (two-way analysis of variance followed by Tukey's *post hoc* test). DCX: doublecortin; SVZ: subventricular zone.

in the majority of cases, and represents an evolutionary strategy to select biological optimization responses (Calabrese and Baldwin, 2001). However, it is likely that the curve response of meloxicam is mainly modulated by a disbalance in the selective inhibition by meloxicam through a higher COX-1/COX-2 ratio, leading to gastrointestinal damage and hepatotoxicity, effects that have previously been linked to an overdose of meloxicam (Zeidler et al., 2002; Adawaren et al., 2018). The lack of systemic anti-inflammatory effect measured by CRP levels in blood with higher doses supports this idea. This U-shaped response makes it difficult to choose the optimal dosage to obtain significant effects and may explain the low number of references on the use of meloxicam as a putative therapy for stroke. However, when administered at the proper dose (which may differ between different experimental models), this agent elicits a very consistent neuroprotection after 48 hours of reperfusion, both in the reduction of infarct volume and improvement of the neurological deficit. In fact, meloxicam presents similar outcomes to those observed with a selective anti-COX-2 agent, celecoxib, the only *coxib* with clear neuroprotective effects in rodent models of stroke (Senda et al., 2011; Santos-Galdiano et al., 2018).

Acute treatment with meloxicam is enough to maintain neuroprotection and modulate the glial scar reactivity after 7 days of reperfusion

Neuroprotective effects similar to those observed after 48 hours were maintained 7 days after the ischemic insult when animals received either acute or chronic treatment with meloxicam. These data show that the two first doses of meloxicam are sufficient to exert a neuroprotective effect maintained over time. However, only animals treated with the chronic dose presented significantly improved behavior. This improvement after the chronic administration could partially rely on meloxicam's ability to reduce post-surgery pain, thus improving the animals' performance in the cylinder test. However, there was a clear tendency for improvement with the acute dose, even when it was not statistically significant. No conclusions can be drawn from the mNSS, as it is only suitable for short reperfusion times because the neurological deficits evaluated have almost disappeared 7 days after ischemic insult.

Astrocyte involvement in the local inflammatory response after ischemia is widely described (Wang et al., 2018, 2020; He et al., 2022), and reactive astrogliosis is a major component of the glial scar. The formation of the glial scar is a double-edged sword; it can limit the extent of the damage, but also interferes with the subsequent neurite regeneration by secreting inhibitory factors (Anderson et al., 2016; Zhou et al., 2020; Koyama and Shichita, 2022). The lack of differences in the morphology of the glial scar between the acute and chronic administrations of meloxicam suggests that the main signals

involved in reactive astrogliosis and glial scar formation are triggered in the first 48 hours. These data match with the time course of two transcription factors involved in astrocyte hypertrophy, i.e., GFAP overexpression and glial scar formation: the nuclear factor kappa B (NF-κB) and signal transducer and activator of transcription (STAT3) pathways (Faulkner et al., 2004; Sofroniew, 2015). NF-κB signaling is activated in the first hours after reperfusion (Stephenson et al., 2000), mainly by pro-inflammatory cytokines (Gorina et al., 2011), leading to the release of interleukin 6, which in turn activates STAT3 (Harré et al., 2003). STAT3 activation is essential to GFAP overexpression and glial scar formation (Herrmann et al., 2008). STAT3 is activated 2–4 hours after reperfusion (Acarin et al., 2000), and it remains activated 24 hours later (Wu et al., 2018). These data suggest that inflammation in the first hours after a stroke is crucial for the initiation of astrocyte reactivity and glial scar formation and would explain why acute and chronic meloxicam are equally effective in modulating astrocyte reactivity in the cerebral cortex. However, studies focused on the molecular aspects of inflammation should be carried out to elucidate the specific mechanism(s) behind this effect.

The modulation of inflammation affects the regenerative processes after stroke in divergent ways

Mounting evidence suggests that regeneration after stroke is triggered in multiple ways, including new cell generation and the induction of synaptic plasticity (Cirillo et al., 2020; Ma et al., 2021). These two mechanisms can be independently activated depending on the model, the reperfusion timing, and the extrinsic conditions or treatments. Our results show that the modulation of inflammation with meloxicam increases axonal sprouting next to the infarcted area, but reduces neurogenesis in the SVZ. The basis underlying the increase in axonal sprouting elicited by meloxicam treatment could be related to the observed reduction of astrocyte reactivity. Axonal sprouting is part of the tissue reorganization and scar formation (Carmichael et al., 2017; Kugler et al., 2020). Complete ablation of the glial scar prevents axonal outgrowth, suggesting that the presence of a glial scar and astrocyte reactivity are necessary for axonal regeneration (Anderson et al., 2016; Liddelow and Barres, 2016); however, excessive astrocyte activation could lead to the axonal outgrowth inhibition (Barreto et al., 2012; Sofroniew, 2015). In this study, meloxicam's effects on the glial scar correlate with increased axonal sprouting, which can be easily attributed to an attempt of the tissue to promote the regeneration of lost connections.

Besides its positive effect on axonal sprouting, meloxicam treatment decreases the generation of newborn neurons in the SVZ. The considerable variability in the data obtained seems to be responsible for the lack of significant differences between the meloxicam chronic treatment compared

to vehicle-treated animals, probably due to the inherent variability in the extent of the infarct volume of this model. However, the observed tendency suggests that NPC formation is triggered in the first 48 hours since both acute and chronic treatments decrease NPC formation. This effect has also been reported in non-pathological conditions in both the SVZ and the subgranular zone in healthy animals treated with meloxicam (Goncalves et al., 2010), and similar effects have been reported in COX-2 KO mice (Sasaki et al., 2003). The influence of COX inhibition on neurogenesis is not fully understood, but it has been related to the decrease of prostaglandins such as prostaglandin E2 (PGE2). PGE2 transactivates a receptor for the ependymal growth factor triggering the mitotic signaling (Pai et al., 2002). Thus, inhibition of PGE2 by anti-inflammatory agents could account for decreased mitotic signaling and a reduction in the division of NPCs (Sasaki et al., 2003). The strong effect of meloxicam on inhibiting PGE2 production (Li et al., 2016) could explain these results. Another possible mechanism could rely on the reduction of microglia reactivity by meloxicam, since microglia-derived factors stimulate the early stages of neurogenesis and promote NPC recruitment to the sites of inflammation (Whitney et al., 2009; Bye et al., 2012). A third mechanism could involve the neurotransmitter gamma-aminobutyric acid (GABA). GABAergic signaling blocks cell proliferation, while GABAergic inhibition increases NPC proliferation and differentiation (Pallotto and Deprez, 2014). A study carried out in a hippocampal slice culture model of ischemia showed that meloxicam promotes the expression of GABA receptors, suggesting a putative role of meloxicam in increasing GABAergic signaling (Landucci et al., 2018). All these mechanisms are plausible and may participate in the inhibition of neurogenesis after meloxicam treatment. Whether this inhibition is detrimental or irrelevant to the recovery after stroke is a matter to be analyzed in further studies accounting for longer times of reperfusion.

The surprising similarities in the response after acute and chronic administration of meloxicam support the high relevance of short-term treatment of inflammation. Moreover, it shows that the modulation of inflammation in early time points impacts later events of regeneration processes, such as axonal sprouting and neurogenesis. This modulation presents special relevance in the search for putative therapies for stroke since many studies, focused only on providing neuroprotection by reducing the infarct volume, do not consider the effects on regenerative attempts. The tight connection between inflammation and regeneration makes it imperative to study these events after experimental anti-inflammatory treatments.

There are some limitations in the present study. First, this study was performed exclusively in male rats and the results should not be automatically assumed to be similar in females. To accurately state that this effect is equally observed in females specific experiments should be carried out. Second, the markers that we utilized to analyze astroglia and microglia are traditional markers (GFAP and IBA-1 respectively) that have been demonstrated recently not label all the phenotypically diversity of astrocytes and microglia (Westergard and Rothstein, 2020; Paolicelli et al., 2022). In terms of image analysis, the large area covered by stroke made the brain slices very fragile, and even though we maximized the preservation of the slice, some regions were too fragile which led in some cases to the loss of small fragments in the immunostaining. Lastly, we only investigated the long-term effects at 7 days post-ischemia, while the axonal sprouting and other regenerative pathways can be active further than this studied timepoint.

In summary, this study shows for the first time the dosage effect of meloxicam treatment after a transient stroke model, and how this neuroprotective effect is linked to both the promotion and the reduction of different regenerative events that occur after stroke. In summary, this study provides a perspective analysis of the use of anti-inflammatory treatments after stroke and how these treatments should be carefully analyzed in the short and long term after stroke.

Author contributions: Concept, design, experimental studies, data acquisition and analysis, statistical analysis, manuscript preparation: IFU. Experimental studies, data acquisition, and manuscript review: PGR. Experimental studies, data acquisition, and manuscript review: MSG. Experimental studies, data acquisition, and manuscript review: EFB. Concept, manuscript review: BAS. Concept, design, data analysis tools, manuscript editing and review: DPR. Concept and design: JMGO. Concept, design, definition of intellectual content, manuscript editing and review: AFL. All authors approved the final version of the paper.

Conflicts of interest: The authors declare no conflicts of interest.

Author statement: This paper has been posted as a preprint on bioRxiv with doi: <https://doi.org/10.1101/2021.04.05.438505> before submitting, which is available from: <https://www.biorxiv.org/content/10.1101/2021.04.05.438505v1>.

Data availability statement: No additional data are available.

Open access statement: This is an open access journal, and articles are distributed under the terms of the Creative Commons AttributionNonCommercial-ShareAlike 4.0 License, which allows others to remix, tweak, and build upon the work non-commercially, as long as appropriate credit is given and the new creations are licensed under the identical terms.

References

- Acarin L, González B, Castellano B (2000) STAT3 and NFκB activation precedes glial reactivity in the excitotoxically injured young cortex but not in the corresponding distal thalamic nuclei. *J Neuropathol Exp Neurol* 59:151-163.
- Adawaren EO, Mukandiwa L, Njaya EM, Bekker L, Duncan N, Naidoo V (2018) The use of liver slices from the Cape vulture (*Gyps coprotheres*) to better understand the role of liver toxicity of non-steroidal anti-inflammatory drugs (NSAIDs) in vultures. *Environ Toxicol Pharmacol* 62:147-155.
- Anderson MA, Burda JE, Ren Y, Ao Y, O'Shea TM, Kawaguchi R, Coppola G, Khakh BS, Deming TJ, Sofroniew MV (2016) Astrocyte scar formation AIDS central nervous system axon regeneration. *Nature* 532:195-200.
- Anrather J, Iadecola C (2016) Inflammation and stroke: an overview. *Neurotherapeutics* 13:661-670.
- Anuncibay-Soto B, Pérez-Rodríguez D, Santos-Galdiano M, Font-Belmonte E, Ugidos IF, Gonzalez-Rodriguez P, Regueiro-Purriños M, Fernández-López A (2018) Salubrinal and robenacoxib treatment after global cerebral ischemia. Exploring the interactions between ER stress and inflammation. *Biochem Pharmacol* 151:126-137.
- Banerjee A, McCullough LD (2022) Sex-specific immune responses in stroke. *Stroke* 53:1449-1459.
- Barreto G, E. White R, Ouyang Y, Xu L, G. Giffard R (2012) Astrocytes: Targets for neuroprotection in stroke. *Cent Nerv Syst Agents Med Chem* 11:164-173.
- Bekker A, Kloopping C, Collingwood S (2018) Meloxicam in the management of post-operative pain: Narrative review. *Anaesthesiol Clin Pharmacol* 34:450-457.
- Bye N, Turnley AM, Morganti-Kossmann MC (2012) Inflammatory regulators of redirected neural migration in the injured brain. *Neurosignals* 20:132-146
- Calabrese EJ, Baldwin LA (2001) U-Shaped dose-responses in biology, toxicology, and public health. *Annu Rev Public Health* 22:15-33.
- Carmichael ST, Kathirvelu B, Schweppe CA, Nie EH (2017) Molecular, cellular and functional events in axonal sprouting after stroke. *Exp Neurol* 287:384-394.
- Choi SH, Aid S, Bosetti F (2009) The distinct roles of cyclooxygenase-1 and-2 in neuroinflammation: implications for translational research. *Trends Pharmacol Sci* 30:174-181
- Cirillo C, Brihmat N, Castel-Lacanal E, Le Fric A, Barbieux-Guillot M, Raposo N, Pariente J, Viguier A, Simonetta-Moreau M, Albuher JF, Olivot JM, Desmoulin F, Marquet P, Chollet F, Loubinoux I (2020) Post-stroke remodeling processes in animal models and humans. *J Cereb Blood Flow Metab* 40:3-22.
- Cruz JV, Rosa JMC, Kimani NM, Giulianti S, Dos Santos CBR (2022) The role of celecoxib as a potential inhibitor in the treatment of inflammatory diseases- A review. *Curr Med Chem* 29:3028-3049.
- Dabrowski A, Robinson TJ, Felling RJ (2019) Promoting brain repair and regeneration after stroke: a plea for cell-based therapies. *Curr Neurol Neurosci Rep* 19:5.
- Dadasheva MN, Gorenkov RV, Zolotovskaya IA, Dadasheva KN (2020) The assessment of the clinical efficacy and tolerability of complex treatment of patients with acute low-back pain. *Zh Nevrol Psikiatr Im S S Korsakova* 120:47-52.
- Dixit A, Pandey P, Dhasmana DC (2020) In vivo effects of nonselective, partially selective, and selective non-steroidal anti-inflammatory drugs on lipid peroxidation and antioxidant enzymes in patients with rheumatoid arthritis: a clinical study. *Int J Appl Basic Med Res* 10:167-172.
- Drieu A, Levard D, Vivien D, Rubio M (2018) Anti-inflammatory treatments for stroke: from bench to bedside. *Ther Adv Neurol Disord* 11:1756286418789854.
- Faki Y, Er A (2021) Different chemical structures and physiological/pathological roles of cyclooxygenases. *Rambam Maimonides Med J* 12:e0003.
- Faulkner JR, Herrmann JE, Woo MJ, Tansey KE, Doan NB, Sofroniew MV (2004) Reactive astrocytes protect tissue and preserve function after spinal cord injury. *J Neurosci* 24:2143-2155.
- Franklin RJM, Simons M (2022) CNS remyelination and inflammation: From basic mechanisms to therapeutic opportunities. *Neuron* 110:3549-3565.
- Ghazanfari N, van Waarde A, Dierckx R, Doorduyn J, de Vries EFJ (2021) Is cyclooxygenase-1 involved in neuroinflammation? *J Neurosci Res* 99:2976-2998.
- Goncalves MB, Williams EJ, Yip P, Yáñez-Muñoz RJ, Williams G, Doherty P (2010) The COX-2 inhibitors, meloxicam and nimesulide, suppress neurogenesis in the adult mouse brain. *Br J Pharmacol* 159:1118-1125.
- Gorina R, Font-Nieves M, Márquez-Kisinousky L, Santalucia T, Planas AM (2011) Astrocyte TLR4 activation induces a proinflammatory environment through the interplay between MyD88-dependent NFκB signaling, MAPK, and Jak1/Stat1 pathways. *Glia* 59:242-255.
- Gundersen HJ, Bagger P, Bendtsen TF, Evans SM, Korbo L, Marcussen N, Møller A, Nielsen K, Nyengaard JR, Pakkenberg B, Sørensens FB, Vesterby A, West MJ (1988) The new stereological tools: disector, fractionator, nucleator and point sampled intercepts and their use in pathological research and diagnosis. *APMS* 96:857-881.
- Gupta YK, Chaudhary G, Sinha K (2002) Enhanced protection by melatonin and meloxicam combination in a middle cerebral artery occlusion model of acute ischemic stroke in rat. *Can J Physiol Pharmacol* 80:210-217.
- Harré EM, Roth J, Gerstberger R, Hübschle T (2003) Interleukin-6 mediates lipopolysaccharide-induced nuclear STAT3 translocation in astrocytes of rat sensory circumventricular organs. *Brain Res* 980:151-155.
- Hawkey CJ (1999) COX-2 inhibitors. *Lancet* 353:307-314.

- He T, Yang GY, Zhang Z (2022) Crosstalk of astrocytes and other cells during ischemic stroke. *Life (Basel)* 12:910.
- Herrmann JE, Imura T, Song B, Qi J, Ao Y, Nguyen TK, Korsak RA, Takeda K, Akira S, Sofroniew MV (2008) STAT3 is a critical regulator of astrogliosis and scar formation after spinal cord injury. *J Neurosci* 28:7231-7243.
- Horgan MD, Knych HK, Siksay SE, Duerr RS (2020) Pharmacokinetics of a single dose of oral meloxicam in rehabilitated wild brown pelicans (*Pelecanus occidentalis*). *J Avian Med Surg* 34:329-337.
- Jacobsen KR, Fauerby N, Raida Z, Kallikoski O, Hau J, Johansen FF, Abelson KS (2013) Effects of buprenorphine and meloxicam analgesia on induced cerebral ischemia in C57BL/6 male mice. *Comp Med* 63:105-113.
- Jayaraj RL, Azimullah S, Beiram R, Jalal FY, Rosenberg GA (2019) Neuroinflammation: Friend and foe for ischemic stroke. *J Neuroinflammation* 16:142.
- Jiang Y, Liu Z, Liao Y, Sun S, Dai Y, Tang Y (2022) Ischemic stroke: From pathological mechanisms to neuroprotective strategies. *Front Neurol* 13:1013083.
- Ju Z, Li M, Xu J, Howell DC, Li Z, Chen FE (2022) Recent development on COX-2 inhibitors as promising anti-inflammatory agents: The past 10 years. *Acta Pharm Sin B* 12:2790-2807.
- Kaur N, Chugh H, Sakharkar MK, Dhawan U, Chidambaram SB, Chandra R (2020) Neuroinflammation mechanisms and phytotherapeutic intervention: a systematic review. *ACS Chem Neurosci* 11:3707-3731.
- Kawasaki A, Okada M, Tamada A, Okuda S, Nozumi M, Ito Y, Kobayashi D, Yamasaki T, Yokoyama R, Shibata T, Nishina H, Yoshida Y, Fujii Y, Takeuchi K, Igarashi M (2018) Growth cone phosphoproteomic reveals that GAP-43 phosphorylated by JNK is a marker of axon growth and regeneration. *iScience* 4:190-203.
- Koyama R, Shichita T (2022) Glial roles in sterile inflammation after ischemic stroke. *Neurosci Res* doi: 10.1016/j.neures.2022.10.002.
- Kugler C, Thielscher C, Tambe BA, Schwarz MK, Halle A, Bradke F, Petzold GC (2020) Epthilones improve axonal growth and motor outcomes after stroke in the adult mammalian CNS. *Cell Rep Med* 1:100159.
- Kunz T, Marklund N, Hillered L, Oliw EH (2002) Cyclooxygenase-2, prostaglandin synthases, and prostaglandin H2 metabolism in traumatic brain injury in the rat. *J Neurotrauma* 19:1051-1064.
- Landucci E, Llorente IL, Anuncibay-Soto B, Pellegrini-Giampietro DE, Fernández-López A (2018) Bicuculline reverts the neuroprotective effects of meloxicam in an oxygen and glucose deprivation (OGD) model of organotypic hippocampal slice cultures. *Neuroscience* 386:68-78.
- Lascelles BDX, Blikslager AT, Fox SM, Reece D (2005) Gastrointestinal tract perforation in dogs treated with a selective cyclooxygenase-2 inhibitor: 29 Cases (2002-2003). *J Am Vet Med Assoc* 227:1112-1117.
- Li T, Zhong J, Dong X, Xiu P, Wang F, Wei H, Wang X, Xu Z, Liu F, Sun X, Li J (2016) Meloxicam suppresses hepatocellular carcinoma cell proliferation and migration by targeting COX-2/PGE2-regulated activation of the β -catenin signaling pathway. *Oncol Rep* 35:3614-3622.
- Liddelow SA, Barres BA (2016) Regeneration: Not everything is scary about a glial scar. *Nature* 532:182-183.
- Ma Y, Yang S, He Q, Zhang D, Chang J (2021) The role of immune cells in post-stroke angiogenesis and neuronal remodeling: the known and the unknown. *Front Immunol* 12:784098.
- Morrison HW, Filosa JA (2013) A quantitative spatiotemporal analysis of microglia morphology during ischemic stroke and reperfusion. *J Neuroinflammation* 10:4.
- Otani K, Shichita T (2020) Cerebral sterile inflammation in neurodegenerative diseases. *Inflamm Regen* 40:28.
- Paciaroni M, Caso V, Agnelli G (2009) The concept of ischemic penumbra in acute stroke and therapeutic opportunities. *Eur Neurol* 61:321-330.
- Pai R, Soreghan B, Szabo IL, Pavelka M, Baatar D, Tarnawski AS (2002) Prostaglandin E2, transactivates EGF receptor: A novel mechanism for promoting colon cancer growth and gastrointestinal hypertrophy. *Nat Med* 8:289-293.
- Pairet M, Van Ryn J, Mauz A, Schierok H, Diederer W, Türck D, Engelhardt G (1998) Differential inhibition of COX-1 and COX-2 by NSAIDs: a summary of results obtained using various test systems. In: *Selective COX-2 Inhibitors* (Vane J, Botting J, eds), pp 27-46. Springer Netherlands.
- Pallotto M, Deprez F (2014) Regulation of adult neurogenesis by GABAergic transmission: signaling beyond GABA_A-receptors. *Front Cell Neurosci* 8:166.
- Paolicelli RC, Sierra A, Stevens B, Tremblay ME, Aguzzi A, Ajami B, Amit I, Audinat E, Bechmann J, Bennett M, Bennett F, Bessis A, Biber K, Bilbo S, Blurton-Jones M, Boddeke E, Brites D, Bröne B, Brown GC, Butovsky O, et al. (2022) Microglia states and nomenclature: A field at its crossroads. *Neuron* 110:3458-3483.
- Passarelli JP, Nimjee SM, Townsend KL (2022) Stroke and neurogenesis: bridging clinical observations to new mechanistic insights from animal models. *Transl Stroke Res* doi: 10.1007/s12975-022-01109-1.
- Paxinos G, Watson C (2006) *The rat brain in stereotaxic coordinates*. San Diego: Academic Press.
- Percie du Sert N, Hurst V, Ahluwalia A, Alam S, Avey MT, Baker M, Browne WJ, Clark A, Cuthill IC, Dirnagl U, Emerson M, Garner P, Holgate ST, Howells DW, Karp NA, Lázic SE, Lidster K, MacCallum CJ, Macleod M, Pearl EJ, et al. (2020) The ARRIVE guidelines 2.0: Updated guidelines for reporting animal research. *PLoS Biol* 18:e3000410.
- Pereira MA, Campos KD, Gonçalves LA, dos Santos RS, Flôr PB, Ambrósio AM, Otsuki DA, Matera JM, Gomes CO, Fantoni DT (2021) Cyclooxygenases 1 and 2 inhibition and analgesic efficacy of dipyrone at different doses or meloxicam in cats after ovariohysterectomy. *Vet Anaesth Analg* 48:7.
- Pluta R, Januszewski S, Czuczwar SJ (2021) Neuroinflammation in post-ischemic neurodegeneration of the brain: friend, foe, or both? *Int J Mol Sci* 22:4405.
- Pu H, Hayashi K, Andras IE, Eum SY, Hennig B, Toborek M (2007) Limited role of COX-2 in HIV Tat-induced alterations of tight junction protein expression and disruption of the blood-brain barrier. *Brain Res* 1184:333-344.
- Radenovic L, Nenadic M, Ufamek-Kozioł M, Januszewski S, Czuczwar SJ, Andjus PR, Pluta R (2020) Heterogeneity in brain distribution of activated microglia and astrocytes in a rat ischemic model of Alzheimer's disease after 2 years of survival. *Aging (Albany NY)* 12:12251-12267.
- Saad J, Mathew D (2022) *Nonsteroidal anti-inflammatory drugs toxicity*. StatPearls. Treasure Island (FL): StatPearls Publishing.
- Santos-Galdiano M, Pérez-Rodríguez D, Anuncibay-Soto B, Font-Belmonte E, Ugidos IF, Pérez-García CC, Fernández-López A (2018) Celecoxib treatment improves neurologic deficit and reduces selective neuronal loss and glial response in rats after transient middle cerebral artery occlusion. *J Pharmacol Exp Ther* 367:528-542.
- Sasaki E, Tominaga K, Watanabe T, Fujiwara Y, Oshitani N, Matsumoto T, Higuchi K, Tarnawski AS, Arakawa T (2003) COX-2 is essential for EGF induction of cell proliferation in gastric RGM1 cells. *Dig Dis Sci* 48:2257-2262.
- Schoos A, Chantziaras I, Vandenabeele J, Biebut E, Meyer E, Cools A, Devreese M, Maes D (2020) Prophylactic use of meloxicam and paracetamol in periparturient sows suffering from postpartum dysgalactia syndrome. *Front Vet Sci* 7:603719.
- Sekeljc V, Bataveljic D, Stamenkovic S, Ufamek M, Jabłoński M, Radenovic L, Pluta R, Andjus PR (2012) Cellular markers of neuroinflammation and neurogenesis after ischemic brain injury in the long-term survival rat model. *Brain Struct Funct* 217:411-420.
- Senda DM, Franzin S, Mori MA, Oliveira RMWd, Milani H (2011) Acute, post-ischemic sensorimotor deficits correlate positively with infarct size but fail to predict its occurrence and magnitude after middle cerebral artery occlusion in rats. *Behav Brain Res* 216:29-35.
- Shahjouei S, Cai PY, Ansari S, Shariffar S, Azari H, Ganji S, Zand R (2016) Middle cerebral artery occlusion model of stroke in rodents: a step-by-step approach. *J Vasc Interv Neurol* 8:1-8.
- Sofroniew MV (2015) Astrocyte barriers to neurotoxic inflammation. *Nat Rev Neurosci* 16:372.
- Stephenson D, Yin T, Smalstig EB, Hsu MA, Panetta J, Little S, Clemens J (2000) Transcription factor nuclear factor-kappa B is activated in neurons after focal cerebral ischemia. *J Cereb Blood Flow Metab* 20:592-603.
- Stiller CO, Hjemdahl P (2022) Lessons from 20 years with COX-2 inhibitors: importance of dose-response considerations and fair play in comparative trials. *J Intern Med* 292:557-574.
- Trueman RC, Diaz C, Farr TD, Harrison DJ, Fuller A, Tokarczuk PF, Stewart AJ, Paisley SJ, Dunnett SB (2017) Systematic and detailed analysis of behavioural tests in the rat middle cerebral artery occlusion model of stroke: Tests for long-term assessment. *J Cereb Blood Flow Metab* 37:1349-1361.
- Tsuyama J, Nakamura A, Ooboshi H, Yoshimura A, Shichita T (2018) Pivotal role of innate myeloid cells in cerebral post-ischemic sterile inflammation. *Semin Immunopathol* 40:523-538.
- Ugidos IF, Santos-Galdiano M, Pérez-Rodríguez D, Anuncibay-Soto B, Font-Belmonte E, López DJ, Ibarra M, Busquets X, Fernández-López A (2017) Neuroprotective effect of 2-hydroxy arachidonic acid in a rat model of transient middle cerebral artery occlusion. *J Cereb Blood Flow Metab* 37:1349-1361.
- Wang H, Song G, Chuang H, Chiu C, Abdelmaksoud A, Ye Y, Zhao L (2018) Portrait of glial scar in neurological diseases. *Int J Immunopathol Pharmacol* 31:2058738418801406.
- Wang J, Sareddy GR, Lu Y, Pratap UP, Tang F, Greene KM, Meyre PL, Tekmal RR, Vadlamudi RK, Brann DW (2020) Astrocyte-derived estrogen regulates reactive astrogliosis and is neuroprotective following ischemic brain injury. *J Neurosci* 40:9751-9771.
- Westergard T, Rothstein JD (2020) Astrocyte Diversity: Current Insights and Future Directions. *Neurochem Res* 45:1298-1305.
- Whitney NP, Eidem TM, Peng H, Huang Y, Zheng JC (2009) Inflammation mediates varying effects in neurogenesis: Relevance to the pathogenesis of brain injury and neurodegenerative disorders. *J Neurochem* 108:1343-1359.
- Wu Y, Xu J, Xu J, Zheng W, Chen Q, Jiao D (2018) Study on the mechanism of JAK2/STAT3 signaling pathway-mediated inflammatory reaction after cerebral ischemia. *Mol Med Rep* 17:5007-5012.
- Zeidler H, Kaltwasser JP, Leonard JP, Kohlmann T, Sigmund R, Degner F, Hettich M (2002) Prescription and tolerability of meloxicam in day-to-day practice: Postmarketing observational cohort study of 13,307 patients in Germany. *J Clin Rheumatol* 8:305-315.
- Zhou Y, Shao A, Yao Y, Tu S, Deng Y, Zhang J (2020) Dual roles of astrocytes in plasticity and reconstruction after traumatic brain injury. *Cell Commun Signal* 18:62.

C-Editors: Zhao M, Liu WJ; S-Editor: Li CH; L-Editors: Li CH, Song LP; T-Editor: Jia Y